DOI: 10.18287/2541-7525-2025-31-1-75-85

Response simulation and primary vertex reconstruction in the SPD NICA straw tracker

Morozova*[1] *S.D.*, *Shipilova*[1,2] *A.V.

[1] *Samara National Research University, Samara, Russian Federation; svtmorozova09@gmail.com; ORCID: 0009-0009-1168-8529 (S.D.); shipilova.av@ssau.ru; ORCID: 0000-0003-3965-3757 (A.V.);*
[2] *Joint Institute for Nuclear Research, Dubna, Russian Federation;*

Received: *30.01.2025*
Revised: *18.03.2025*
Accepted: *07.04.2025*

Scientific article

Abstract. In this work we investigate the temporal structure of the events in the spin physics detector (SPD) straw tracker at the JINR NICA. Using the Geant4 toolkit we simulate the response of the straw layers sensitive elements in the trigger-free regime of SPD. Using the simulation results we present a simple algorithm for the fast primary-vertex finding and estimate the efficiency and purity of the reconstruction.

Key words: Monte Carlo simulation; track approximation; primary vertex reconstruction; reconstruction efficiency; Geant4; SPD NICA; straw tube; detector.

Introduction

At the present time, the spin structure of the nucleon is one of the challenging topics of high-energy physics. Nowadays, a new accelerator complex, the NICA (Nuclotron based Ion Collider fAcility) collider, is being built at the Joint Institute for Nuclear Research (Dubna, Russia). The Spin Physics Detector (SPD) is proposed to be placed in one of the two interaction points of the NICA to study the nucleon spin structure and other spin-related phenomena with polarized proton and deuteron beams [1]. The SPD physics program is described in detail in [2–4] and mainly aimed to extract information on the gluon Transverse-Momentum-Dependent Parton Distribution Functions (TMD PDFs) in the proton and deuteron, as well as the gluon transversity distribution and tensor PDFs in the deuteron, via the measurement of specific single- and double-spin asymmetries using such complementary probes as charmonia, open charm, and prompt photon production processes. These phenomena are planned to study at the center-of-mass collision energy $\sqrt{s}$ up to 27 GeV and a total luminosity up to 10^{32} cm^{-2} s^{-1}. Since the $\sqrt{s}$ exceeds the typical hard scale of the studied processes moderately, the 4π geometry resolution of the SPD is planned, together with triggerless data acquisition system (DAQ), purposed to minimize systematic uncertainties of the measurements. For the effective data recognition under specified conditions, the related software should provide fast data processing, event selection, and primary vertex reconstruction at the online data filtering stage. Particularly, for the rational use of memory and high-performance the simplest procedure of track fitting and further primary vertex recovery is anticipated [5–7].

1. Straw tracker simulation

The straw tracker (ST) is the inner part of the SPD detector aimed at reconstructing tracks of primary and secondary particles with high efficiency for the precise measurements of their momenta and to identify particles via their energy deposition. Its construction includes the barrel part and two end-caps [1], constituted of two different kinds of the low-mass straw tubes, similar to those used in such modern experiments as NA64 [8], COMPASS [9; 10] and others [1]. The most of the produced particles will be registered in the barrel part consisting of the 8 azimuthal modules, each containing the 31 double layers of straw tubes, which schematic view is presented at the Fig. 1 [1].

The geometrical ST model used in this study was developed by A. Allakhverdieva using the GeoModel toolkit [11; 12], which is a class library for the description of detector geometry. The designed ST geometry is stored in the local GeoModel SQLite file (.db) being the input of the Geant4 package [13–15], generating the detector model automatically. Such an approach for the detector simulation provides the flexibility of the model, simplifying the purely construction changes. To describe the ST geometry, we use a global coordinate system, where the z-axis is oriented along the nominal beam direction, the y-axis is vertical, and the x-axis is perpendicular to them and is directed toward the center of the collider ring. The origin of the coordinate system is the nominal center of the setup being the ideal interaction point. The ST model of the present study is specified by the setup with inner and outer radii of 270 and 867 mm, respectively, consisting of 8 octants filled with layers of cylindrical tubes, to be shown in the XOY plane in the Fig. 2. The base of the detector, the ST tubes, are constructed from a thick polyethylene shell and an inner cylindrical volume of radius R = 4.78 mm filled by the gas mixture of $Ar(70\%) + CO_2(30\%)$. The internal volume of each tube is represented by the GEANT4 sensitive detector object ConstructSDandField and the HitsCollection array, which elements (Hits) are recorded every time a particle looses energy in the sensitive volume, and contain information about the particle type, energy loss, coordinates, track data, and the unique number of the tube where the hit is arised.

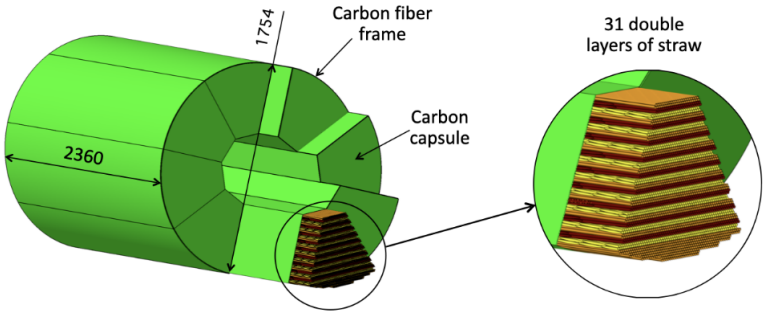

Fig. 1. Schematic representation of the Straw Tracker (ST) [1]
Рис. 1. Схематичное представление строу-трекера (ST) [1]

2. Experiment simulation

We consider the p-p mode of the experiment where the proton beams collide at the energy of $\sqrt{s} = 27$ GeV in the center-of-mass system. We suppose the proton bunch crossing every 76 ns, while the temporal interval of the data storing (timeslice), defined by the DAQ system, to be 10 μs. The heavy charged primary particles are simulated by positive muons with a given energy of $E = 1$ GeV and momentum $\vec{p}$, which direction has a uniform spatial distribution, using the G4PrimaryVertex object of the Geant4. The such choice of primary particles has been made due to their small cross section of interaction with ST material resulting the small number of secondary tracks while the major energy loss of a muon is due to a gas ionization, which is favourable to initiate the electron avalanche into a straw drift chamber.

The probability of a hard interaction between two protons in a given beam crossing is simulated by the Poisson distribution $f(k) = \frac{\lambda^k}{k!} e^{-\lambda}$ with the expected value $\lambda = 0.3$. We impose the coordinates of the interaction point and the corresponding primary vertex to be the same and equal to $(0, 0, z)$, where z is normally distributed around the central value $z_0 = 0$ by a Gaussian distribution $f(z) = \frac{1}{\sigma\sqrt{2\pi}} e^{-\frac{1}{2}\left(\frac{z-z_0}{\sigma}\right)^2}$ with $\sigma = 30$ cm. The number of muons produced in the one pp hard interaction is determined by a Poisson distribution with the expected value $\lambda = 7$. The propagation of a charged particle through a gas leads to energy loss due to ionization. The snapshot of the

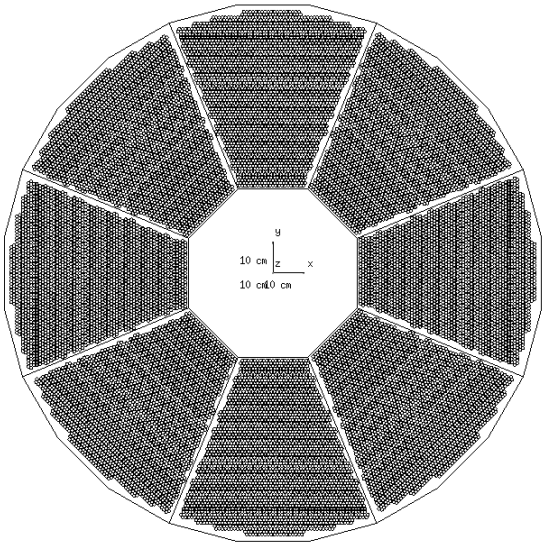

Fig. 2. The ST model used in this work in *XOY* plane

Рис. 2. Модель строу-трекера, используемая в представленной работе, в плоскости *XOY*

particle state at the moment of energy loss within the sensitive volume was recorded as a hit. The visualization of launch of one event into the ST is shown in Fig. 3, where the hits and tracks are illustrated by green dots and blue lines, respectively.

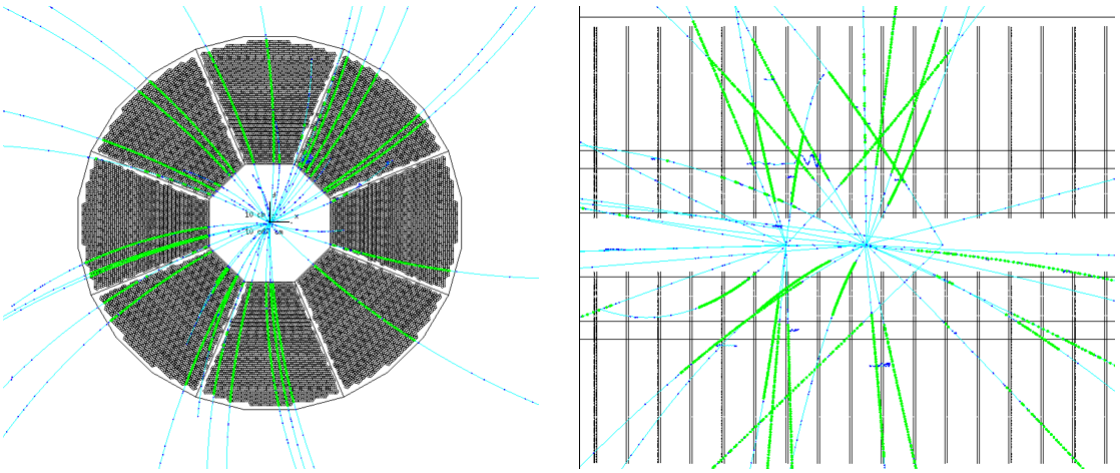

Fig. 3. Visualization of launch of one event into the ST: *XOY* plane (left), *ZOY* plane (right). Hits and tracks are illustrated by green dots and blue lines, respectively (see the color online on the wersite)

Рис. 3. Визуализация запуска одного события в строу-трекере: в плоскости *XOY* (слева), в плоскости *ZOY* (справа). Зеленые точки — точки потери энергии в чувствительном объеме, голубые линии — треки (цвет см. в онлайн-варианте на сайте)

We collected the hits into hit arrays applying the following selection criteria: only the energy loss of primary particles were considered with the threshold for the total energy loss of $E_{tot} > 100$ MeV, and all the secondary particles are neglected. The set of coordinates of each muon energy loss points were used to determine the shortest distance to the tube axis, anode wire, to calculate the response time of the straw tube. This time depends on the electron avalanche drift time from the ionization point to the anode wire $t(r)$, where r is the shortest distance from the track to the anode. Using

the complete hit collection array for a given muon we can reconstruct its track and apply this procedure for all the muons in the simulation. If there are several points of muon energy loss in one logical volume, we approximate the muon track by a straight line connecting the first and the last hits, then r is calculated as the shortest distance between this line and tube axis. The hit reconstruction step was omitted for the transparency of the simulation results, that means the 3D coordinates of particle hits are assumed to be known. The distance from the hit to the anode wire is calculated using the local coordinates, relatively to the axis of a particular tube, and the tracks are approximated in global coordinates, relative to the entire detector. Since each particle is tracked individually in GEANT4, it is not suitable to simulate interactions for a large number of particles, as the electron avalanche is. Thus, we used the $t(r)$ dependence [1] simulated using the GARFIELD software [16; 17]), for which we found the analytical approximation: $t(r) = 2.7101 + 1.2156r + 6.8287r^2$. We present the resulting temporal distribution averaged by 100 time slices in the Fig. 4, where grey area corresponds to the times of the sensitive volume intersections by the sample particle, and colored area is straw tubes response time distribution. Here and after all the histograms were generated using the CERN ROOT [18] tools. We obtain the significant overlap between the straw tubes response times from the different bunch crossings appearing in the same time slice. This fact indicates the problem of signal decoding for track and primary vertex reconstruction during data collection in a real experiment.

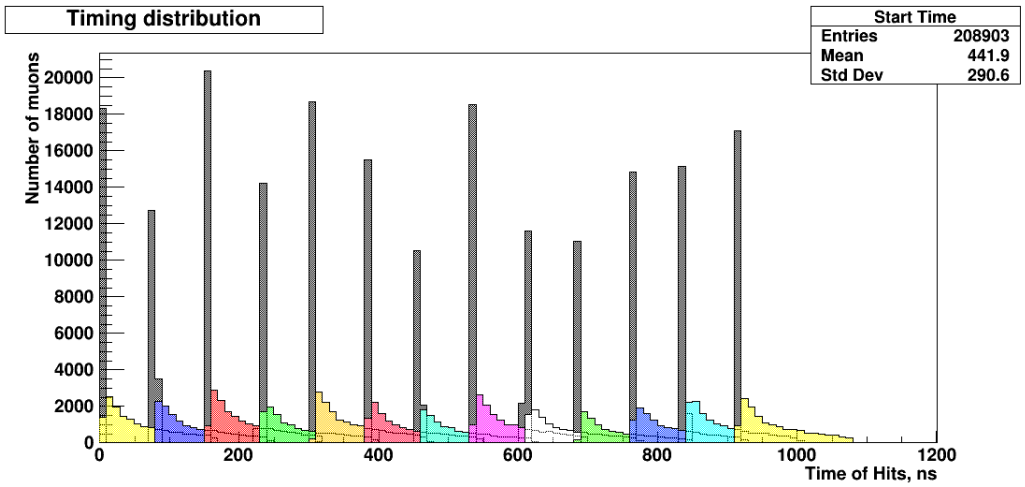

Fig. 4. Temporal distribution averaged by 100 time slices, grey area – times of the sensitive volume intersections by the sample particle, colored area – straw tubes response time distribution

Рис. 4. Временное распределение, усредненное по 100 временным срезам. Серая область – время пересечения чувствительного объема частицей из выборки, цветная область – распределение времен отклика строу-трубок

3. Primary vertex reconstruction

To reconstruct primary vertices assigned with bunch crossings points, we develop an algorithm based on the simplest approximation of particle tracks, making it suitable in the online evaluations for the triggerless regime of ST. For the pure examination of the algorithm, we omit the step of hit reconstruction, and reconstruct the tracks using the direct coordinates of the hits collected in Sec. 1. In our simulation we suppose a magnetic field oriented along z-axis to be equal to $B = 1$ T and uniform everywhere inside the ST, providing a spiral trajectory of a charged particle. We approximate the muon motion in the XOY plane by the parabola and a straight line in the ZOX or YOZ planes, see Fig. 3. The set of hits $\{x_i, y_i\}_N$ in the XOY plane for the each track numbered N is approximated by the parabolic function $\tilde{y} = a_{2,N}\tilde{x}^2 + a_{1,N}\tilde{x} + a_{0,N} = f(\tilde{x})$ where the coefficients $a_{i,N}$ are determined using the least-squares method. Since the system has a rotational symmetry in the XOY plane, but the coordinate system is fixed, we should choose the desired approximation

function to be $Y(X)$ or $X(Y)$ for the each track. It is done by the following procedure: if any of the sets $\{x_i\}_N, \{y_i\}_N$ is not ordered by ascending or descending, its elements correspond to function values $\tilde{y}(\tilde{x})$ while the elements of another to argument values $\tilde{x}$. In the case whether both sets are ordered, the adjusted R square values are calculated using the following formulas:

$$R^2_{Adj} = 1 - \frac{(1-R^2)(k-1)}{k-n-1} \qquad R^2 = 1 - \frac{\sum\limits_{i=1}^{k}(y_i - f(x_i))^2}{\sum\limits_{i=1}^{k}(y_i - \bar{y})^2}. \tag{1}$$

Then we compare values of R^2_{Adj} for $\{x_i, y_i\}_N$ corresponding to choices $(\tilde{x}, \tilde{y})$ and $(\tilde{y}, \tilde{x})$ to adopt one providing the higher R^2_{Adj}.

The coefficients a_i for each primary particle determine the arc length of the parabolic segment L_N which is calculated using a simple formula

$$\begin{aligned} L_N(\tilde{x}_{i,N}) &= \int_0^{\tilde{x}_{i,N}} \sqrt{1 + (f'(\tilde{x}))^2}d\tilde{x} = \\ &= \frac{1}{4a_{2,N}}\left(\ln\left|\sqrt{(f'(\tilde{x}_{i,N}))^2 + 1} + f'(\tilde{x}_{i,N})\right| + f'(\tilde{x}_{i,N})\sqrt{(f'(\tilde{x}_{i,N}))^2 + 1}\right). \end{aligned} \tag{2}$$

Then we can use it to obtain the dependence $z(L)_N = b_{1,N}L_N + b_{0,N}$, where $z(L)_N$ can be approximated by a linear function, which must be extrapolated to intersect with the Z-axis in order to determine the position of the primary vertex. The simulated tracks and hits in the ZOY plane from the primary particles in one time slice are shown in Fig. 3.

The coordinates of the hit are approximated assuming that the particle is produced at the point $\{0, 0, Z_0\}$. The approximated tracks are passed then through the two selection criteria. The first one is based on the polar angle θ of the track, which is determined as the angle between the line connecting the start point of the track with the first hit and the Z axis.

Analysing the distribution of the vertex reconstruction error by polar angle, we can conclude that particle tracks close to Z-axis do not intersect a sufficient number of detector layers, resulting a decrease in the reconstruction accuracy, since the extrapolation error multiplies the approximation error. Therefore, we decided to exclude all tracks with polar angle $\theta < 0.5$ and $\theta > \pi - 0.5$, and this reduces the number of tracks to 80 % from the initial one. In the Fig. 5 we present the distance distribution between the reconstructed vertex and the true vertex depending on the polar angle.

The second track selection criterion is derived by the RSS (regression residuals squares) parameter value stated by the formula:

$$RSS_z = \sum_{i=1}^{n}(z_{i,N} - (b_{0,N} + b_{1,N}L_N(\tilde{x}_{i,N})))^2. \tag{3}$$

Tracks with an RSS below the value of 1.0 are discarded. This critical value was chosen as corresponding to the optimal ratio of discarded to actually poorly reconstructed tracks, leading to the 56% of the remaining from the initial number of tracks.

The obtained distortion of the distribution relative to $\theta = \pi$, see Fig. 5, is due to the asymmetry of the trajectories of positive muons propagating in and against the direction of the magnetic induction lines. Assuming the $Z_0 - Z_{nach}$ data are normally distributed within a certain range of θ values, we defined the parameters of Gaussian distribution corresponding to the each θ interval:

$$f(Z_0, \theta) = \frac{1}{\sigma(\theta)\sqrt{2\pi}} e^{-\frac{1}{2}\left(\frac{Z_0 - \mu(\theta)}{\sigma(\theta)}\right)^2}. \tag{4}$$

The obtained parameters $\mu(\theta)$ and $\sigma(\theta)$ will be used for further track processing. The obtained dependence of the standard deviation and the mean value on the polar angle is shown in Fig. 6.

Using the mean value, the reconstructed Z_0s were corrected. The $\sigma(\theta)$ is the corresponding reconstruction error of a particular vertex, which was used for vertex clustering and for

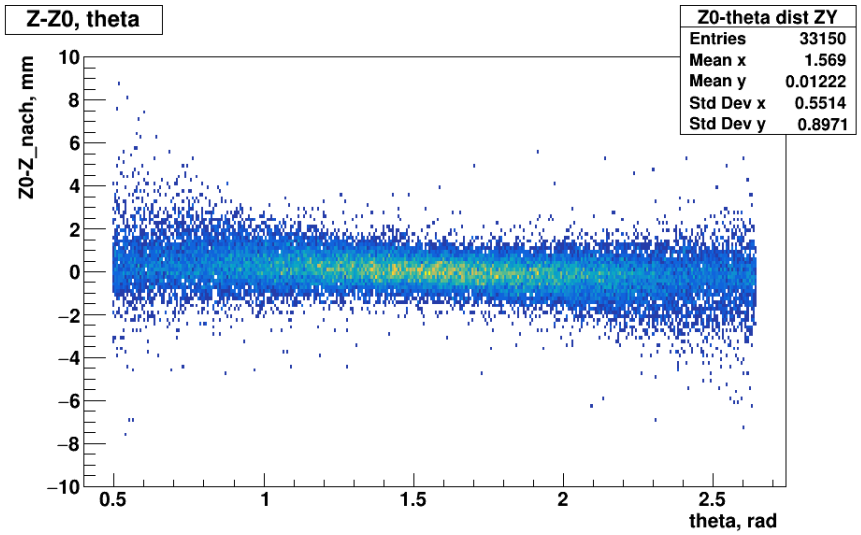

Fig. 5. Distance distribution between the reconstructed vertex and the true vertex versus the polar angle θ

Рис. 5. Распределение расстояния между реконструированной вершиной и истинной вершиной в зависимости от полярного угла θ

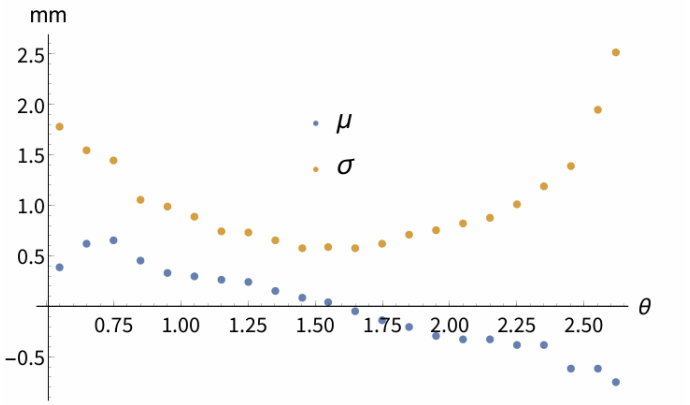

Fig. 6. Dependence of the standard deviation (σ) and the mean value (μ) on the polar angle

Рис. 6. Зависимость стандартного отклонения (σ) и среднего значения (μ) от полярного угла (θ)

correcting the reconstructed vertices. The adjusted distance distribution between the reconstructed vertex and the true vertex are shown in Fig. 7.

The next step is to group the tracks into clusters with common vertices expected as primary vertices. The set of initial coordinate values Z_0 was sorted in ascending order. The reconstructed Z_0 values were taken into account with a corresponding error interval $\{Z_{0,k} \pm \sigma_k\}$. In case error intervals overlap, all Z_0s in a given region are considered as one cluster treated as reconstructed primary vertex with the coordinate $Z_{0,C} = \frac{1}{K}\sum_{k=1}^{K} Z_{0,k}$. After all the clusters has been found by this procedure we compare their coordinates with true primary vertices. In case of two or more vertices are present within a single cluster they are combined into one primary vertex only if the distance between them does not exceed $3\sigma_0$, where $\sigma_0 = 1$ mm. If several vertices within a cluster are at a greater distance, they are all considered to be reconstructed incorrectly. A correctly reconstructed vertex is one that can be distinguished in the cluster, and all assigned tracks actually belong to it. To determine this, we used the ID of the track (TrackID), which is matched between the reconstructed and true vertex in this algorithm. Among all the incorrectly reconstructed vertices N_{wr} the fraction related to indistinguishability $\frac{N_{wr.vert}}{N_{wr}} = 96$ %. The vertex reconstruction efficiency was calculated as the

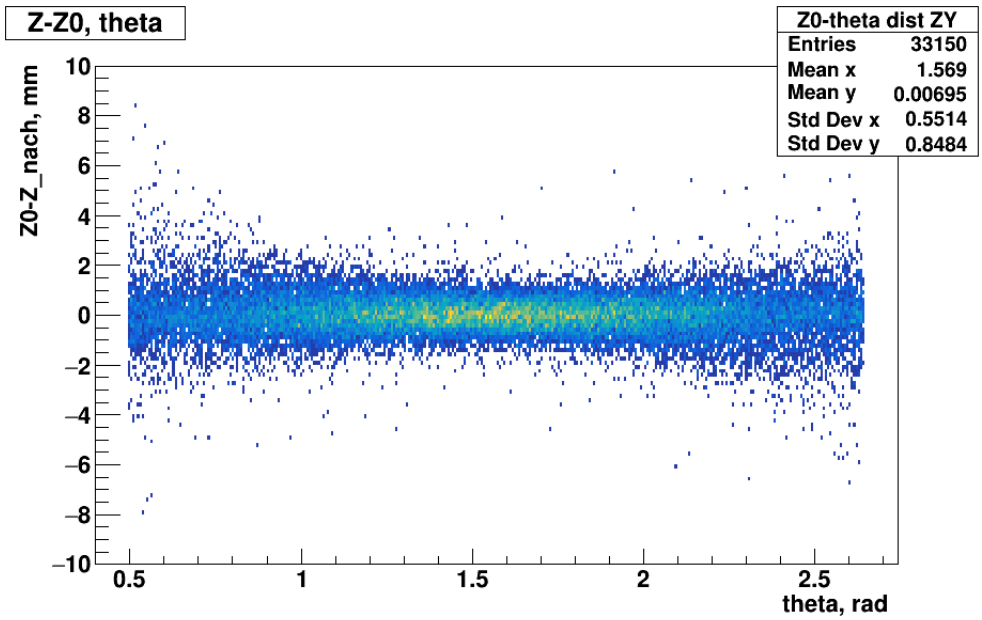

Fig. 7. Adjusted distribution of the distance between the reconstructed vertex and the true vertex versus polar angle θ

Рис. 7. Скорректированное распределение расстояния между реконструированной вершиной и истинной вершиной в зависимости от полярного угла θ

ratio of the number of correctly reconstructed true vertices to the total number of true vertices in the dataset. The efficiency obtained by this method is $\frac{N_{reco}}{N_{all}} = 97.1$ %.

As a result, if the initial vertices are far enough apart each other, they are easily distinguishable and can be correctly reconstructed. However, if the primary vertices are closely located, the error regions in the reconstructed Z_0 can overlap, reducing the efficiency of the reconstruction process.

In the Fig. 8, left, we present the dependence of primary vertex reconstruction efficiency which is defined as the ratio of all the reconstructed vertices to the all initial true vertices in the simulation, against the critical value of the RSS_z parameter. While on the right panel we demonstrate the percentage of the vertices lost by use the RSS_z-related criterion. One can find the maximal efficiency is achieved at the $RSS_z = 1$ being equal to 77.1 %.

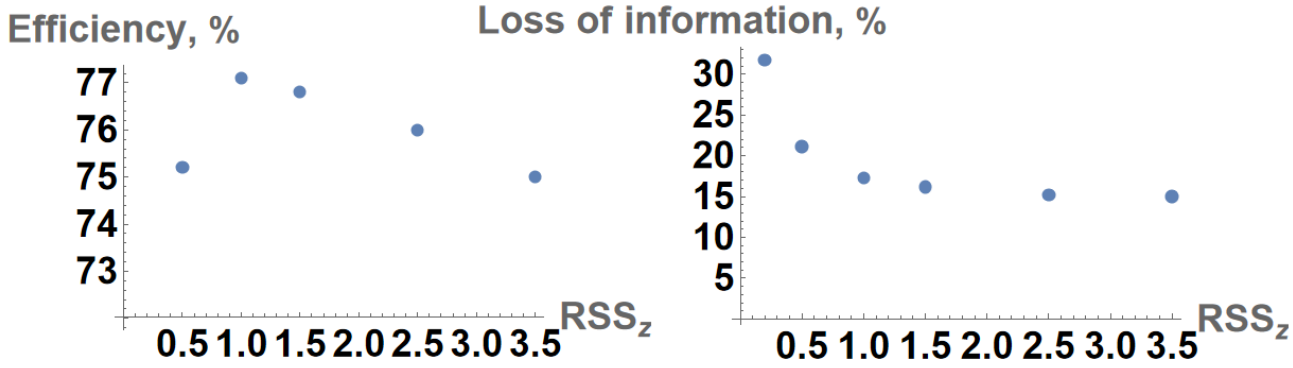

Fig. 8. Efficiency dependence (left) and vertices information loss (right) on RSS_z of $z(l)$ approximation

Рис. 8. Зависимость эффективности реконструкции вершин (слева) и потери информации о вершинах (справа) от порогового значения RSS_z аппроксимации $z(l)$

Conclusions

We present the algorithm for the primary vertex reconstruction in the SPD NICA straw tracker which gives an opportunity to resolve a complicated temporal structure of the ST response within the timeslice. Due to the simplicity of the algorithm it is fast and can be used for the online data processing in the triggerless regime of the detector operation. We found the optimal parameters providing the maximal efficiency with minimal information loss, and a good quality of the vertex reconstruction on the conditionally-reduced sample of the true vertices.

The further study implies the verification of the algorithm performance using the hit data with less purity and using more complicated functions for track approximations.

Funding. The work was supported by the state assignment of the Ministry of Science and Higher Education of the Russian Federation, № FSSS-2025-0003.

Acknowledgements: the authors are grateful to A. Allahverdiyeva for providing the detector model, to I.I. Denisenko, A.S. Zhemchugov and other participants of the SPD NICA Collaboration for useful comments and fruitful discussions.

Information about the conflict of interests: authors and reviewers declared no conflicts of interest.

Citation. Morozova S.D., Shipilova A.V. Response simulation and primary vertex reconstruction in the SPD NICA straw tracker. *Vestnik Samarskogo universiteta. Estestvennonauchnaya seriya / Vestnik of Samara University. Natural Science Series*, 2025, vol. 31, no. 1, pp. 75–85. DOI: 10.18287/2541-7525-2025-31-1-75-85.

Svetlana D. Morozova (svtmorozova09@gmail.com) – Master's degree student of the Department of General and Theoretical Physics, Samara National Research University, 34, Moskovskoye shosse, 443086, Russian Federation.

Aleksandra V. Shipilova (shipilova.av@ssau.ru) – Candidate of Physical and Mathematical Sciences, assistant professor of the Department of General and Theoretical Physics, Samara National Research University, 34, Moskovskoye shosse, Samara, 443086, Russian Federation; senior research fellow, Joint Institute for Nuclear Research, 6, Joliot-Curie Street, Dubna, 141980, Russian Federation.

References

[1] Abazov V. [et al.] Technical Design Report of the Spin Physics Detector at NICA. *Natural Science Review*, 2024, vol. 1, p. 1. URL: https://nsr-jinr.ru/index.php/nsr/article/view/35.

[2] Abazov V.M. [et al.] Conceptual design of the Spin Physics Detector. arXiv: 2102.00442. DOI: https://doi.org/10.48550/arXiv.2102.00442.

[3] Arbuzov A. [et al.] On the physics potential to study the gluon content of proton and deuteron at NICA SPD. *Progress in Particle and Nuclear Physics*, 2021, vol. 119, P. 103858. DOI: https://doi.org/10.1016/j.ppnp.2021.103858.

[4] Abramov V.V. [et al.] Possible Studies at the First Stage of the NICA Collider Operation with Polarized and Unpolarized Proton and Deuteron Beams. *Physics of Particles and Nuclei*, 2021, vol. 52, issue 6, pp. 1044–1119. DOI: https://doi.org/10.1134/S1063779621060022.

[5] Andreev V.F. Comparison of Algorithms for Reconstructing the Primary Interaction Vertex for the SPD Experiment. *Bulletin of the Lebedev Physics Institute*, 2021, vol. 48, pp. 301–306. DOI: https://doi.org/10.3103/S106833562110002X.

[6] Andreev V.F., Gerassimov S.G., Terkulov A.R. Software for Tracks and Primary Vertex Reconstruction for the SPD Experiment. *Physics of Particles and Nuclei*, 2021, vol. 52, pp. 793–796. DOI: https://doi.org/10.1134/S1063779621040055.

[7] Morozova S.D., Shipilova A.V. The Simulation of Interactions in the Straw-Based SPD Track Detector and Primary Vertex Reconstruction. *Physics of Particles and Nuclei Letters*, 2024, vol. 21, pp. 727–730. DOI: https://doi.org/10.1134/S154747712470119X.

[8] Volkov V. [et al.] Straw Chambers for the NA64 Experiment. *Physics of Particles and Nuclei Letters*, 2019, vol. 16, pp. 847–858. DOI: 10.1134/S1547477119060554.

[9] Bychkov V. [et al.] Construction and manufacture of large size straw-chambers of the COMPASS spectrometer tracking system. *Particles and Nuclei, Letters*, 2002, no. 2 (111), pp. 64–73. Available at: https://inis.iaea.org/records/38dge-vqj08.

[10] Platzer K. [et al.] Mapping the large area straw detectors of the COMPASS experiment with Xrays. *IEEE Transactions on Nuclei Science*, 2005, vol. 52, issue 3, pp. 793–98. DOI: http://doi.org/10.1109/NSSMIC.2004.1462189.

[11] Merkt S.A. [et al.] Going standalone and platform-independent, an example from recent work on the ATLAS Detector Description and interactive data visualization. *EPJ Web of Conferences*, 2019, vol. 214, p. 02035. DOI: https://doi.org/10.1051/epjconf/201921402035.

[12] Bandieramonte M., Bianchi R. M., Boudreau J., Dell'Acqua A., Tsulaia V. The new GeoModel suite, a lightweight detector description and visualization toolkit for HEP. *Journal of Physics Conference Series*, 2023, vol. 2438, p. 012051. DOI: https://doi.org/10.1088/1742-6596/2438/1/012051.

[13] Agostinelli S. [et al.] GEANT4 – a simulation toolkit. *Nuclear Instruments and Methods in Physics Research Section A: Accelerators, Spectrometers, Detectors and Associated Equipment*, 2003, vol. 506, issue 3, pp. 250–303. DOI: https://doi.org/10.1016/S0168-9002(03)01368-8.

[14] Allison J. [et al.] Geant4 developments and applications. *IEEE Transactions on Nuclei Science*, 2006, vol. 53, issue 1, pp. 270–278. DOI: https://doi.org/10.1109/TNS.2006.869826.

[15] Allison J. [et al.] Recent developments in Geant4. *Nuclear Instruments and Methods in Physics Research Section A: Accelerators, Spectrometers, Detectors and Associated Equipment*, 2016 vol. 835, pp. 186–225. DOI: https://doi.org/10.1016/j.nima.2016.06.125.

[16] Veenhof R. Garfield, a drift chamber simulation program. *Conference Proceedings*, 1993, C 9306149, pp. 66–71. Available at: https://inspirehep.net/literature/370078.

[17] Veenhof R. GARFIELD, recent developments. *Nuclear Instruments and Methods in Physics Research Section A: Accelerators, Spectrometers, Detectors and Associated Equipment*, 1998, vol. 419, pp. 726–730. DOI: https://doi.org/10.1016/S0168-9002(98)00851-1.

[18] Brun R., Rademakers F. ROOT – An Object Oriented Data Analysis Framework. *Nuclear Instruments and Methods in Physics Research Section A: Accelerators, Spectrometers, Detectors and Associated Equipment*, 1997, vol. 389, pp. 81–86. DOI: https://doi.org/10.1016/s0168-9002(97)00048-x.

DOI: 10.18287/2541-7525-2025-31-1-75-85 УДК 539.1; 621.384.6

Моделирование отклика и восстановление первичных вершин в трековом строу-детекторе SPD NICA

Морозова*[1] *С.Д.*, *Шипилова*[1,2] *А.В.

[1] *Самарский национальный исследовательский университет имени академика С.П. Королева, г. Самара, Российская Федерация; svtmorozova09@gmail.com; ORCID: 0009-0009-1168-8529 (С.Д.); shipilova.av@ssau.ru; ORCID: 0000-0003-3965-3757 (А.В.);*
[2] *Объединенный институт ядерных исследований, г. Дубна, Российская Федерация;*

Поступила: *30.01.2025*
Рассмотрена: *18.03.2025*
Принята: *07.04.2025*

Научная статья

Аннотация. В данной работе мы изучаем временную структуру событий в строу-детекторе спиновой физики (SPD) ускорителя NICA в ОИЯИ. С помощью программного пакета Geant4 мы моделируем отклик чувствительных элементов слоев строу-трубок при бестриггерном режиме работы SPD. Используя результаты моделирования, мы представляем простой алгоритм быстрого поиска первичных вершин и оцениваем его эффективность и чистоту реконструкции.

Ключевые слова: Монте-Карло моделирование; аппроксимация треков; реконструкция первичных вершин; эффективность восстановления; Geant4; SPD NICA; строу-трубка; детектор.

Финансирование. Работа выполнена в рамках государственного задания Министерства науки и высшего образования Российской Федерации, № FSSS-2025-0003.

Благодарность: авторы выражают благодарность А. Аллахвердиевой за предоставленную модель детектора, И.И. Денисенко, А.С. Жемчугову и другим участникам коллаборации SPD NICA за полезные замечания и плодотворные обсуждения.

Информация о конфликте интересов: авторы и рецензенты заявляют об отсутствии конфликта интересов.

Цитирование. Morozova S.D., Shipilova A.V. Response simulation and primary vertex reconstruction in the SPD NICA straw tracker // Вестник Самарского университета. Естественнонаучная серия / Vestnik of Samara University. Natural Science Series 2025. Т. 31, № 1. С. 75–85. DOI: 10.18287/2541-7525-2025-31-1-75-85.

Светлана Денисовна Морозова (svtmorozova09@gmail.com) – магистрант кафедры общей и теоретической физики, Самарский национальный исследовательский университет имени академика С.П. Королева, 443086, Российская Федерация, г. Самара, Московское шоссе, 34.
Александра Викторовна Шипилова (shipilova.av@ssau.ru) – кандидат физико-математических наук, доцент кафедры общей и теоретической физики, Самарский национальный исследовательский университет имени академика С.П. Королева, 443086, Российская Федерация, г. Самара, Московское шоссе, 34; старший научный сотрудник, Объединенный институт ядерных исследований, 141980, Российская Федерация, г. Дубна, ул. Жолио-Кюри, 6.

Литература

[1] Abazov V. [et al.] Technical Design Report of the Spin Physics Detector at NICA // Natural Science Review. 2024. Vol. 1. P. 1. Available at: https://nsr-jinr.ru/index.php/nsr/article/view/35.

[2] Abazov V.M. [et al.] Conceptual design of the Spin Physics Detector. arXiv: 2102.00442. DOI: https://doi.org/10.48550/arXiv.2102.00442.

[3] Arbuzov A. [et al.] On the physics potential to study the gluon content of proton and deuteron at NICA SPD // Progress in Particle and Nuclear Physics. 2021. Vol. 119. P. 103858. DOI: https://doi.org/10.1016/j.ppnp.2021.103858.

[4] Abramov V.V. [et al.] Possible Studies at the First Stage of the NICA Collider Operation with Polarized and Unpolarized Proton and Deuteron Beams // Physics of Particles and Nuclei. 2021. Vol. 52, issue 6. P. 1044–1119. DOI: https://doi.org/10.1134/S1063779621060022.

[5] Andreev V.F. Comparison of Algorithms for Reconstructing the Primary Interaction Vertex for the SPD Experiment // Bulletin of the Lebedev Physics Institute. 2021. Vol. 48. P. 301–306. DOI: https://doi.org/10.3103/S106833562110002X.

[6] Andreev V.F., Gerassimov S.G., Terkulov A.R. Software for Tracks and Primary Vertex Reconstruction for the SPD Experiment // Physics of Particles and Nuclei. 2021. Vol. 52. P. 793–796. DOI: https://doi.org/10.1134/S1063779621040055.

[7] Morozova S.D., Shipilova A.V. The Simulation of Interactions in the Straw-Based SPD Track Detector and Primary Vertex Reconstruction // Physics of Particles and Nuclei Letters. 2024. Vol. 21. P. 727–730. DOI: https://doi.org/10.1134/S154747712470119X.

[8] Volkov V. [et al.] Straw Chambers for the NA64 Experiment // Physics of Particles and Nuclei Letters. 2019. Vol. 16. P. 847–858. DOI: http://doi.org/10.1134/S1547477119060554.

[9] Bychkov V. [et al.] Construction and manufacture of large size straw-chambers of the COMPASS spectrometer tracking system // Particles and Nuclei, Letters. 2002. № 2 (111). P. 64–73. URL: https://inis.iaea.org/records/38dge-vqj08.

[10] Platzer K. [et al.] Mapping the large area straw detectors of the COMPASS experiment with Xrays // IEEE Transactions on Nuclei Science. 2005. Vol. 52, issue 3. P. 793–98. DOI: http://doi.org/10.1109/NSSMIC.2004.1462189.

[11] Merkt S.A. [et al.] Going standalone and platform-independent, an example from recent work on the ATLAS Detector Description and interactive data visualization // EPJ Web of Conferences. 2019. Vol. 214. P. 02035. DOI: https://doi.org/10.1051/epjconf/201921402035.

[12] Bandieramonte M., Bianchi R.M., Boudreau J., Dell'Acqua A., Tsulaia V. The new GeoModel suite, a lightweight detector description and visualization toolkit for HEP // Journal of Physics Conference Series. 2023. Vol. 2438. P. 012051. DOI: https://doi.org/10.1088/1742-6596/2438/1/012051.

[13] Agostinelli S. [et al.] GEANT4 – a simulation toolkit // Nuclear Instruments and Methods in Physics Research Section A: Accelerators, Spectrometers, Detectors and Associated Equipment. 2003. Vol. 506, issue 3. P. 250–303. DOI: https://doi.org/10.1016/S0168-9002(03)01368-8.

[14] Allison J. [et al.] Geant4 developments and applications // IEEE Transactions on Nuclei Science. 2006. Vol. 53, issue 1. P. 270–278. DOI: https://doi.org/10.1109/TNS.2006.869826.

[15] Allison J. [et al.] Recent developments in Geant4 // Nuclear Instruments and Methods in Physics Research Section A: Accelerators, Spectrometers, Detectors and Associated Equipment. 2016. Vol. 835. P. 186–225. DOI: https://doi.org/10.1016/j.nima.2016.06.125.

[16] Veenhof R. Garfield, a drift chamber simulation program // Conference Proceedings. 1993. C 9306149. P. 66–71. Available at: https://inspirehep.net/literature/370078.

[17] Veenhof R. GARFIELD, recent developments // Nuclear Instruments and Methods in Physics Research Section A: Accelerators, Spectrometers, Detectors and Associated Equipment. 1998. Vol. 419. P. 726–730. DOI: https://doi.org/10.1016/S0168-9002(98)00851-1.

[18] Brun R., Rademakers F. ROOT – An Object Oriented Data Analysis Framework // Nuclear Instruments and Methods in Physics Research Section A: Accelerators, Spectrometers, Detectors and Associated Equipment. 1997. Vol. 389. P. 81–86. DOI: https://doi.org/10.1016/s0168-9002(97)00048-x.